

# Competition between $\text{TiCl}_4$ Hydrolysis and Oxidation and its Effect on Product $\text{TiO}_2$ Powder

M. Kamal Akhtar, Srinivas Vemury, and Sotiris E. Pratsinis

Dept. of Chemical Engineering, Center for Aerosol Processes, University of Cincinnati, Cincinnati, OH 45221

*The competition between hydrolysis and oxidation of  $\text{TiCl}_4$  during vapor-phase synthesis of titania powders was experimentally investigated. The effects of reactor temperature, reactant mixing and  $\text{H}_2\text{O}/\text{TiCl}_4$  ratio were studied in a hot wall aerosol flow reactor. The presence of water vapor resulted in rounded particles instead of the faceted ones observed in the absence of water; this effect was most pronounced at lower reactor temperatures. Mixing the water and  $\text{TiCl}_4$  vapor streams at low temperature resulted in anatase titania. Larger aggregates with smaller primary particles were observed for powders synthesized in the presence of water vapor. The mixing temperature of the water and  $\text{TiCl}_4$  vapors, as well as the  $\text{H}_2\text{O}/\text{TiCl}_4$  ratios, did not affect the aggregate size or specific surface area. Analysis of micrographs of titania aggregates made in the presence of water revealed that the fractal dimension increased with process temperature.*

## Introduction

The competition between oxidation and hydrolysis of precursor vapors is commonly encountered in flame synthesis of titania and fumed silica. Though these are mature technologies, a fundamental understanding of the role of these chemical routes in determining product particle characteristics is still lacking.

Bautista and Atkins (1991) examined the competition between oxidation and hydrolysis of silicon tetrachloride ( $\text{SiCl}_4$ ) in a diffusion flame burner during manufacture of optical fiber preform. In the low-temperature region of the flame, hydrolysis was the main route for  $\text{SiCl}_4$  conversion, while oxidation was dominant in the high-temperature region. Since particle deposition in lightguide preform fabrication is dominated by thermophoresis, higher deposition efficiency (process yield) was obtained by  $\text{SiCl}_4$  oxidation than hydrolysis.

In other processes such as synthesis of oxide powders in hydrocarbon assisted flames, water vapor is present from hydrocarbon combustion. Frequently, aqueous solutions of additives are sprayed into the flame to control particle morphology and size. The crystallinity of flame-synthesized powders is also affected by the presence of water. Hence, it is important to understand the competition between hydrolysis and oxidation of precursor vapors during particle formation for better control of the characteristics of powders made in the gas phase.

The simultaneous oxidation and hydrolysis of  $\text{TiCl}_4$  is chosen as a model system because of the commercial importance of titania and the innovative applications that have recently been proposed for it. Titania is used primarily in pigments as an opacifier (Mezey, 1966), as catalyst support (Bankmann et al., 1992), and as semiconductor (Chen and Wu, 1990). Recent developments have led to the use of titania as a photocatalyst in the removal of organics from wastewater streams (Ollis et al., 1991) and as an inorganic membrane with potential use in the separations industry (Kumar et al., 1992). In these applications, the particle morphology, size distribution, and phase composition are key powder characteristics which must be controlled.

Titania is produced on a large scale in flame reactors by the "chloride" process (Clark, 1975). In this process,  $\text{TiCl}_4$  vapor, oxygen, and hydrocarbons along with various additives react forming  $\text{TiO}_2$  powder, chlorine, water, and so on. A flame, however, is a complex environment. To deconvolute the effects of water from other chemical effects, high-temperature synthesis of  $\text{TiO}_2$  by  $\text{TiCl}_4$  oxidation was conducted here in a hot wall aerosol flow reactor. This reactor allows operation with controlled temperature, residence time, and mixing of the reactants. This article presents an experimental investigation of the effect of water on the morphology, size, and phase composition of titania powders synthesized by gas-phase oxidation and hydrolysis of  $\text{TiCl}_4$ .

Correspondence concerning this article should be addressed to S. E. Pratsinis.

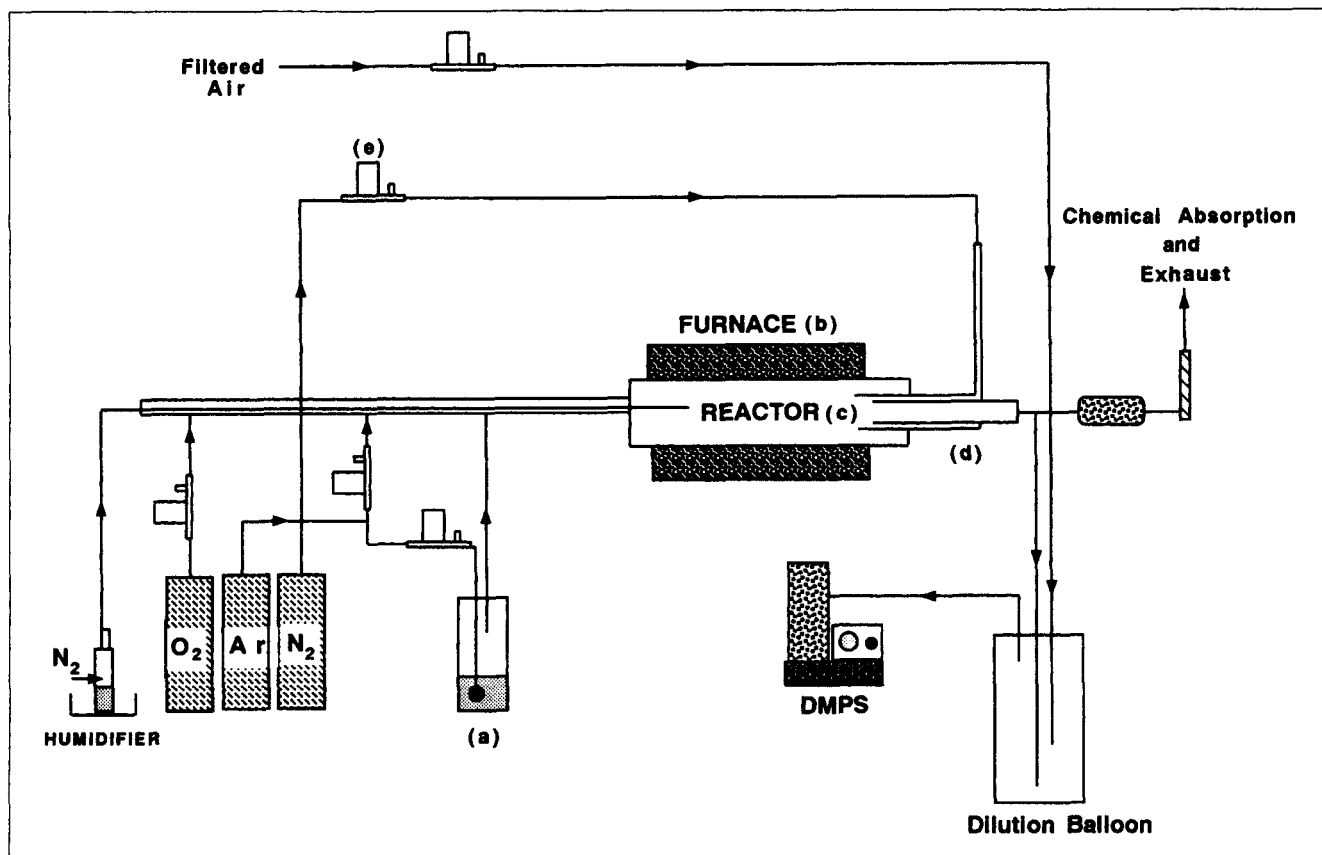


Figure 1. Apparatus used in the synthesis of titania powders in the presence of water vapor.

## Experimental Studies

### Powder synthesis

Titania particles were made at furnace set temperatures of 1,273, 1,473, and 1,673 K, at a reactor residence time of about 1.2 s (at 1,473 K). The precursor  $\text{TiCl}_4$  vapor was introduced into the reactor at a constant rate of  $1.4 \times 10^{-4}$  mol/min during all the experiments, and the molar  $\text{H}_2\text{O}/\text{TiCl}_4$  ratio was varied between 0.03 and 5.07.

A schematic of the experimental apparatus is shown in Figure 1. Clean, dry argon gas (Wright Brothers, 99.8%) is bubbled through a gas-washing bottle (a) containing  $\text{TiCl}_4$  (Aldrich, 99.9%) at room temperature (296 K). The Ar- $\text{TiCl}_4$  vapor stream is diluted with additional argon, mixed with about 10 times the stoichiometric amount of oxygen (Linde, 99.9%) and introduced into the reactor. The reactor is an alumina tube (99.8%  $\text{Al}_2\text{O}_3$ , Coors Ceramics, Inc., 152.4 cm long, 3.175 cm ID) that is externally heated in a horizontal furnace (b, Lindberg 54233). Water droplets generated in nitrogen by a modified home humidifier (Ultra-Mister, Tatung) are carried into the reactor (Lyons et al., 1992) with a ceramic tube (0.317 cm ID, 0.635 cm OD) which is concentric with the  $\text{TiCl}_4$  feed tube (Figure 2). The point of mixing of  $\text{TiCl}_4$  and water vapors is controlled by moving the inner tube along the reactor axis (Figure 2). Powders were synthesized at five mixing points located at various distances ( $a = -4$  cm,  $b = 0$  cm,  $c = 5$  cm,  $d = 8$  cm, and  $e = 13$  cm as shown in Figure 2) from the start (point b) of the furnace. The reactor tube section inside the furnace is 60 cm. The temperature along the reactor axis

increases almost linearly until it reaches a plateau (Figure 3) at the set temperature about 14 cm inside the furnace (Akhtar et al., 1991). Hence, varying the location of the mixing point results in different temperatures of mixing of the  $\text{TiCl}_4$  and water vapors. The inset table in Figure 2 shows the mixing point temperatures for furnace set temperatures used in this study.

The water concentration in the reactor was determined by flowing an aerosol of aqueous NaCl solution (0.05 g/mL) through the reactor. From the inlet droplet NaCl concentration and the weight of NaCl collected on the filter, the amount of water vapor introduced into the reactor was determined (Akhtar, 1993). The concentration of  $\text{TiCl}_4$  in the gas stream was determined by recording the loss in weight of the  $\text{TiCl}_4$ -containing bottle after bubbling argon through it at a flow rate of 200  $\text{cm}^3/\text{min}$ .

The gas stream and entrained product particles are mixed and rapidly cooled with nitrogen in the primary dilutor (d) as they exit the reactor. This quenches particle growth by coagulation outside the reaction zone and reduces thermophoretic losses of particles from the product stream onto the cool dilutor walls. The reactor effluents are further diluted and sampled by the differential mobility particle sizer, collected on filters for further analysis or exhausted through the laboratory hood. All flows into the reactor are precisely controlled by mass-flow controllers (e, 1259B, MKS). A vacuum pump operates downstream at all times to maintain a slight underpressure to ensure stable operation of the humidifier and to assist in particle collection on the filter.

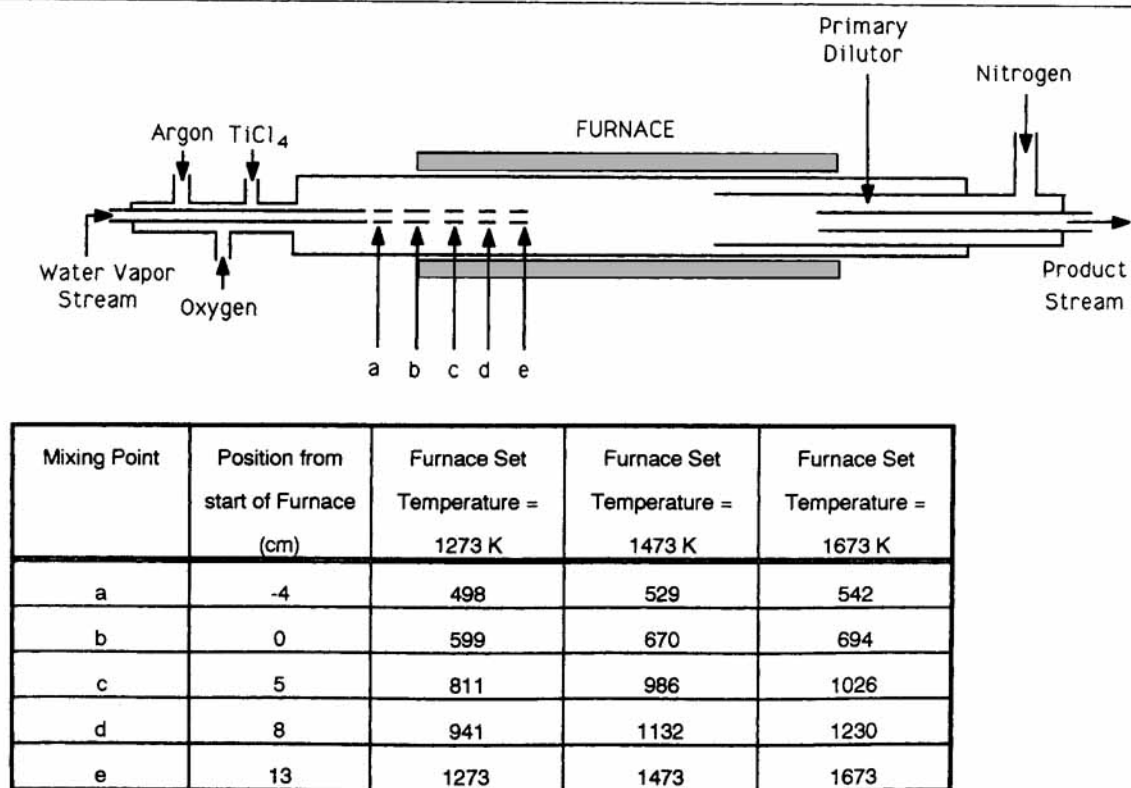


Figure 2. Details of the reactor inlet and outlet arrangements with different mixing points and temperatures.

### Characterization

Transmission electron micrographs (TEM) of the powders were obtained on a Philips CM 20 microscope operating at 160 kV. X-ray photoelectron spectroscopy (Perkin-Elmer) of the powders was conducted to obtain the surface chemical composition.

X-ray diffraction (XRD) was used to determine the phase composition of the titania powders. Samples for XRD analysis were collected on glass fiber filters (Pallaflex), and the diffraction lines were recorded on a diffractometer (D500, Siemens; using  $\text{CuK}\alpha$  radiation). The weight fraction of the anatase and rutile phases in the samples were calculated from the relative intensities of the strongest peaks corresponding to anatase and rutile as described by Spurr and Myers (1957). Crystallite sizes were determined from line broadening measurements using the Scherrer formula (Klug and Alexander, 1954).

The specific surface area of the powder was measured by nitrogen adsorption (Gemini 2360, Micromeritics Inc.) at 77 K using the BET equation. Assuming uniformly sized spherical primary particles within an aggregate, the equivalent average primary particle diameter was calculated:  $d_g = 6/\rho_p A$ , where the anatase titania density  $\rho_p = 3.84 \text{ g/cm}^3$  (Lide, 1990) and  $A$  is the BET specific surface area.

Aggregate particle-size distributions were obtained using the differential mobility particle sizer (DMPS, TSI 3932). The DMPS measures aggregate particle-size distribution by classifying the particles on the basis of their electrical mobility using an electrostatic classifier (TSI 3071) and counting them with a condensation nucleus counter (CNC, TSI 3020). It was difficult to obtain steady operation of the humidifier, while the aerosol was sampled directly from the reactor into the DMPS. Hence, the product stream was sampled into a Mylar balloon filled with clean air and then further diluted to bring the particle number concentration within the measuring limit of the DMPS. The balloon was then attached to the inlet of the DMPS to obtain aggregate particle-size distributions. The

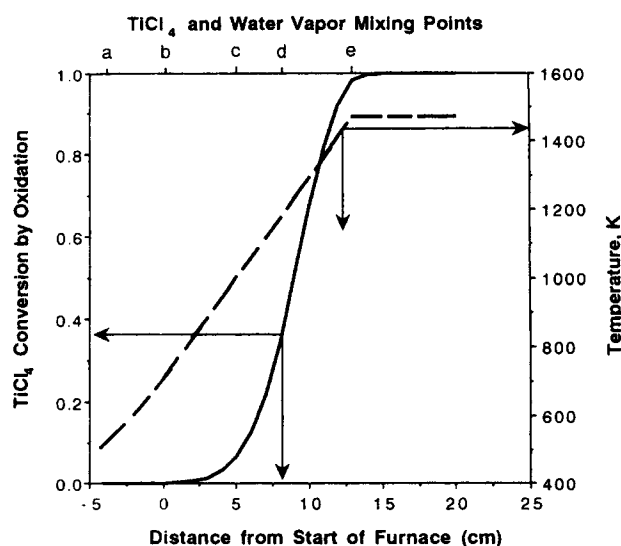
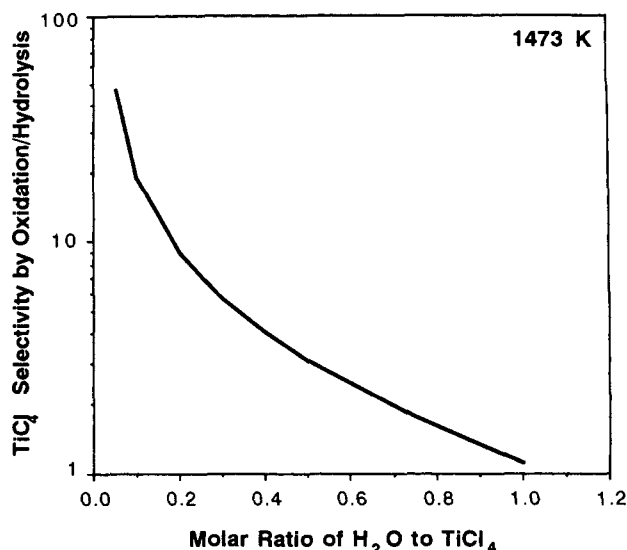


Figure 3.  $\text{TiCl}_4$  conversion as a function of distance from the start of the furnace and corresponding temperatures.

The furnace set temperature was 1,473 K.

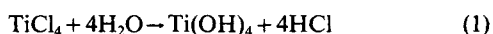


**Figure 4.** Equilibrium calculations showing the relative importance of oxidation and hydrolysis as a function of  $\text{H}_2\text{O}/\text{TiCl}_4$  ratio in the reactant stream.

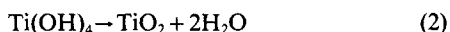
DMPS was operated in the “underpressure” mode with an inlet flow of polydisperse aerosol sample of 0.3 L/min and sheath air flow of 3 L/min. This mode of operation enabled particles between 0.017 and 0.886  $\mu\text{m}$  to be sized.

### Hydrolysis and Oxidation of $\text{TiCl}_4$

In the presence of water and oxygen there are two routes for  $\text{TiCl}_4$  conversion to  $\text{TiO}_2$ : hydrolysis and oxidation. Hydrolysis of  $\text{TiCl}_4$  takes place according to the overall reaction:



At the high temperatures employed in these experiments,  $\text{Ti}(\text{OH})_4$  is converted to  $\text{TiO}_2$ :



Oxidation of  $\text{TiCl}_4$  takes place according to the overall reaction:



The process temperature determines the dominance of  $\text{TiCl}_4$  hydrolysis or oxidation. Titania made by the conversion of  $\text{Ti}(\text{OH})_4$  has a higher anatase content than the powders formed by oxidation as hydrolysis and the resultant formation of the hydroxide can occur even at low temperatures (Oguri et al., 1988).

The conversion of  $\text{TiCl}_4$  by oxidation along the reactor axis is calculated using the temperature profile in Figure 3 for a furnace set temperature of 1,473 K (Pratsinis et al., 1990). Substantial conversion of  $\text{TiCl}_4$  by oxidation takes place only after the first 10 cm of the furnace, where the temperature is sufficiently high. In contrast, hydrolysis can occur even at room temperature. Hence, depending on the  $\text{H}_2\text{O}/\text{TiCl}_4$  ratio

and the location of the mixing point (for example, the initial 10 cm of the furnace: low-temperature zone), hydrolysis can play an important role in  $\text{TiCl}_4$  conversion.

Furthermore, the thermodynamic equilibrium conversion of  $\text{TiCl}_4$  by oxidation and hydrolysis was calculated as a function of water vapor loading (STANJAN: Reynolds, 1987). Figure 4 shows the selectivity of oxidation to hydrolysis route at 1,473 K as a function of  $\text{H}_2\text{O}/\text{TiCl}_4$  ratio. Selectivity is defined here as the ratio of moles of  $\text{TiCl}_4$  converted by oxidation to moles of  $\text{TiCl}_4$  converted by hydrolysis. When the amount of water vapor present is low (low  $\text{H}_2\text{O}/\text{TiCl}_4$  ratio), the selectivity of the oxidation route is high. This drops quite fast as the  $\text{H}_2\text{O}/\text{TiCl}_4$  ratio in the reactant stream increases. At high  $\text{H}_2\text{O}/\text{TiCl}_4$  ratios,  $\text{TiCl}_4$  oxidation and hydrolysis become equally important. The thermodynamic equilibrium calculations, when combined with the slow kinetics of  $\text{TiCl}_4$  oxidation at low temperatures, indicate that water vapor may play a significant role in determining the mechanism of titania formation.

## Results and Discussion

### Particle morphology and chemical characterization

Figure 5a shows a TEM micrograph of titania particles made at furnace set temperature of 1,473 K,  $\text{H}_2\text{O}/\text{TiCl}_4$  ratio of 2.57 and the mixing of  $\text{TiCl}_4$  and water vapor streams taking place at the start of the furnace (point b in Figure 2). These are aggregates of fine, round primary particles. Reducing the  $\text{H}_2\text{O}/\text{TiCl}_4$  ratio to 0.06 does not significantly affect the morphology of the particles (Figure 5b). On moving, however, the reactant mixing point to a higher-temperature region (point d in Figure 2, 8 cm from the start of the furnace), more faceted particles are observed (Figure 5c). This effect is most pronounced at the furnace temperature of 1,673 K, reactant mixing at point e (13 cm from the start of the furnace) and  $\text{H}_2\text{O}/\text{TiCl}_4$  ratio of 0.06 (Figure 5d). Most of the particles are faceted, and the presence of water vapor has little effect on particle morphology.

When the water and  $\text{TiCl}_4$  vapor streams are mixed at high temperatures, the rate of  $\text{TiCl}_4$  oxidation is very fast and the role of hydrolysis should be minimal (Figure 3). Even in the case of mixing at point a (4 cm outside the furnace, mixing temperature = 542 K) with a furnace set temperature of 1,673 K more faceted particles are observed than at 1,273 K. This indicates that even when particles are formed by hydrolysis, their passage through the high-temperature region of the furnace allows them to transform into the faceted crystalline form provided the residence time is long enough. Suyama and Kato (1985) and Akhtar et al. (1991, 1992) have shown that titania powders produced in the absence of water are polyhedral, dense particles with well-defined edges. The presence of water, however, may significantly alter particle morphology.

Figures 5c and 5d show TEM micrographs of titania made at a  $\text{H}_2\text{O}/\text{TiCl}_4$  ratio of 0.06 and at furnace set temperatures of 1,473 and 1,673 K, with the mixing point of  $\text{TiCl}_4$  and water vapor streams at 8 and 13 cm, respectively, from the start of the furnace. The average primary particle size for titania made at 1,473 K is 0.04  $\mu\text{m}$ , while that for particles made at 1,673 K is 0.05  $\mu\text{m}$  as determined from TEM micrographs. At the higher temperature, the particles experience a slightly shorter residence time but the sintering rate is much faster thus promoting the growth of primary particles. Hence, aggregates

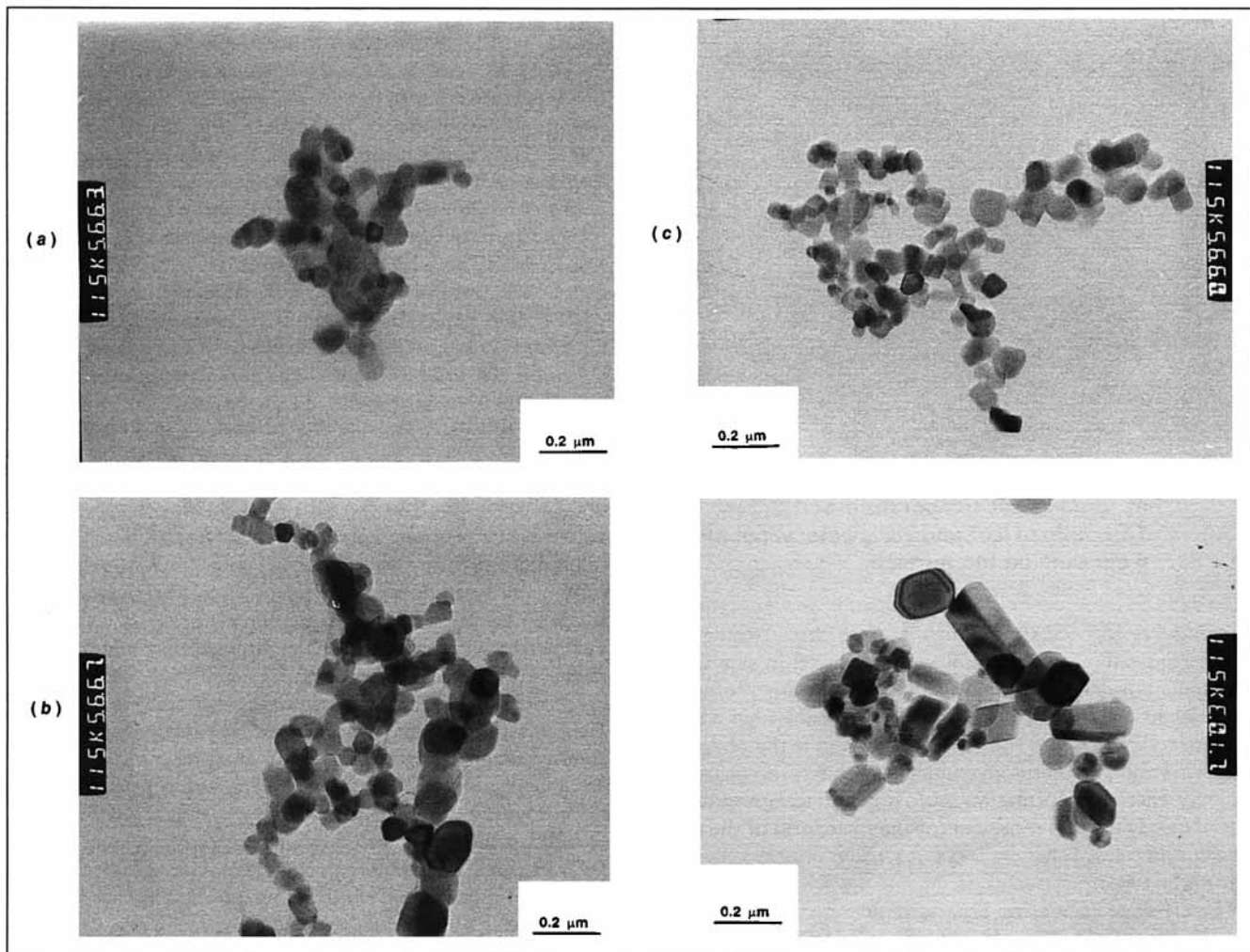


**Figure 5. Micrographs (TEM) of titania particles.**

- (a) Furnace set temperature 1,473 K,  $\text{TiCl}_4$ -water vapor mixing at start of furnace and  $\text{H}_2\text{O}/\text{TiCl}_4$  ratio of 2.57.
- (b) Furnace set temperature 1,473 K,  $\text{TiCl}_4$ -water vapor mixing at start of furnace and  $\text{H}_2\text{O}/\text{TiCl}_4$  ratio of 0.06.
- (c) Furnace set temperature 1,473 K,  $\text{TiCl}_4$ -water vapor mixing 8 cm from the start of the furnace and  $\text{H}_2\text{O}/\text{TiCl}_4$  ratio of 0.06.
- (d) Furnace set temperature 1,673 K,  $\text{TiCl}_4$ -water vapor mixing 13 cm from the start of the furnace and  $\text{H}_2\text{O}/\text{TiCl}_4$  ratio of 0.06.

formed at low temperatures have smaller primary particles than aggregates made at high temperatures.

An interesting morphological feature was observed when the diameter of the feed tube for water vapor was reduced to 0.159 cm and mixing with the  $\text{TiCl}_4$  vapor occurred 4 cm outside the furnace (point a in Figure 2). Interspersed among the typical titania aggregates were spherical particles with smaller particles attached to them. Figure 6 shows a micrograph of these particles made at furnace set temperature of 1,273 K and at  $\text{H}_2\text{O}/\text{TiCl}_4$  ratio of 5.07. The reduction in diameter of the water vapor feed tube increased the volumetric flow rate of water vapor leading to a decrease in the corresponding residence time in the feed tube. Entrained microdroplets from the ultrasonic generator apparently survived the evaporation process and reached inside the reactor. A possible explanation is that the  $\text{TiCl}_4$  vapor reacted may have reacted with these microdroplets resulting in the formation of spherical particles of titania.

The XPS scans of titania made in the presence and absence of water showed only the presence of titanium and oxygen with traces of tin and potassium most probably impurities from the  $\text{TiCl}_4$ . High-resolution scans indicated that only  $\text{TiO}_2$  was present and none of the suboxides of titania were formed. Titanium has several oxidation states but the deconvoluted  $\text{Ti}2p$  spectrum shows the presence of only  $\text{Ti}^{4+}$ . The binding energies of the  $\text{Ti}2p_{3/2}$  and  $\text{Ti}2p_{1/2}$  peaks (467.9 and 462.2 eV) were found to agree very well with the standard values (468.0 and 462.2 eV, Perkin Elmer, 1978).

### Phase composition

Titania exists in three polymorphic forms: rutile (tetragonal,  $P4_2/mnm$ ), anatase (tetragonal,  $I4_1/amd$ ), and brookite (orthorhombic,  $Pcab$ ). Rutile is the only thermodynamically stable form, while anatase and brookite are metastable at all

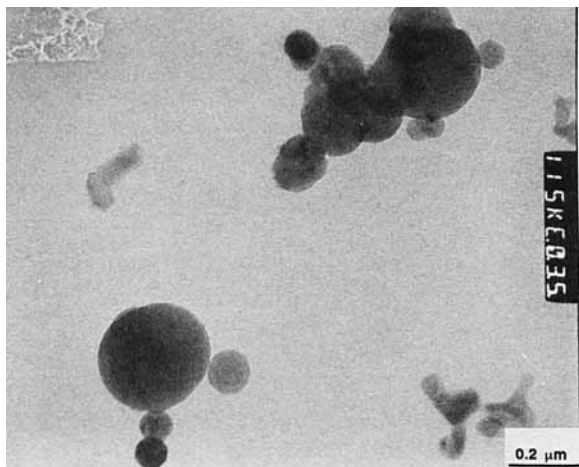


**Figure 6.** Micrographs (TEM) of titania particles made at furnace set temperature of 1,273 K,  $\text{H}_2\text{O}/\text{TiCl}_4$  ratio of 5.07 and  $\text{TiCl}_4$ -water vapor mixing 4 cm outside the furnace.

temperatures and transform to rutile on heating (Rao et al., 1961). Under the process conditions employed in this work, the titania powders are primarily anatase with some rutile but no brookite present (Akhtar et al., 1991). Anatase has a more open structure ( $a = 3.783 \text{ \AA}$ ,  $c = 9.51 \text{ \AA}$ ) and is the phase initially formed. The thermodynamically stable rutile phase has a higher energy of formation and cooperative movement of the  $\text{Ti}^{4+}$  and  $\text{O}^{2-}$  ions is needed for the formation of the more compact ( $a = 4.594 \text{ \AA}$ ,  $c = 2.958 \text{ \AA}$ ) rutile crystal (Shannon and Pask, 1964).

The effect of increasing process temperature on the phase composition of titania powders made at a  $\text{H}_2\text{O}/\text{TiCl}_4$  ratio of 0.06 and reactant gases mixing at point e (13 cm from start of furnace) is shown in Figure 7. The intensity of the primary rutile reflection (110) increases with increasing temperature indicating that the fraction of rutile increases with temperature: from 0 at 1,273 K to about 16% at 1,673 K. The increase in rutile content with increasing temperature is consistent with

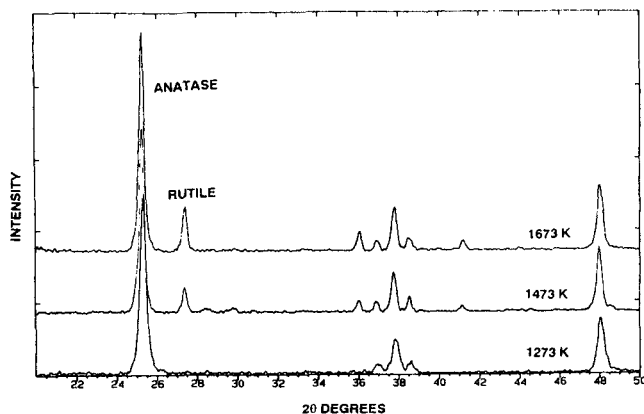


**Figure 7.** XRD patterns for titania made at furnace set temperatures of 1,273, 1,473, and 1,673 K,  $\text{TiCl}_4$ -water vapor mixing 13 cm downstream from the start of the furnace, and  $\text{H}_2\text{O}/\text{TiCl}_4$  ratio of 0.06.

the observations for pure titania (Akhtar et al., 1991) and with the anatase to rutile phase transformation mechanism proposed by Shannon and Pask (1964). At higher temperatures, the cooperative movement of  $\text{Ti}^{4+}$  and  $\text{O}^{2-}$  ions involves the rupture of two of the six Ti-O bonds to form new bonds. The rate of bond breakup is enhanced at the higher temperatures resulting in faster transformation to the rutile phase.

Figure 8a shows the effect of  $\text{TiCl}_4$  and water vapor mixing on the rutile content of titania at set furnace temperatures of 1,273, 1,473, and 1,673 K and  $\text{H}_2\text{O}/\text{TiCl}_4$  ratio of 0.26. In general, the rutile content increases as the temperature is increased and the reactant mixing point is moved closer to the high-temperature zone of the furnace. At 1,273 K set temperature, all the product crystalline powder is anatase and the mixing point has little effect on the phase composition. At a mixing point 4 cm outside the furnace (a in Figure 2), the temperature is low (542 K for a furnace set temperature of 1,673 K), and this results in hydrolysis of  $\text{TiCl}_4$  to form hydrous titania. These powders, on passing through the high-temperature reactor lose two water molecules (Eq. 2) and crystallize to the anatase form. If the residence time and temperature are sufficiently high, then some of the powders are further transformed into rutile. As the mixing point is progressively moved further into the furnace, the temperature at the point of mixing of the water and  $\text{TiCl}_4$  streams increases (1,673 K at 13 cm inside the furnace for a set temperature of 1,673 K) and more  $\text{TiCl}_4$  is oxidized than is hydrolyzed. The powders, formed at high temperatures, are anatase and on further heating during their passage through the reactor a fraction is transformed to rutile. Oguri et al. (1988) and Hebrard et al. (1990) also observed that titania produced by low-temperature hydrolysis of  $\text{TiCl}_4$  is either amorphous or anatase and crystallizes into a mixture of anatase and rutile on further heat treatment.

For mixing of the water and  $\text{TiCl}_4$  streams 4 cm outside the furnace (a in Figure 2), almost all of the powder is probably formed by hydrolysis and is primarily anatase. For reactant mixing further downstream, the role of oxidation becomes dominant and at a mixing point 13 cm from the start of the furnace (e in Figure 2) 16% rutile is observed in the powder. The latter value agrees with the amount of rutile observed in titania powders made in the absence of water (Akhtar et al., 1991). This confirms that high furnace set temperatures and mixing of  $\text{TiCl}_4$  and water vapor streams in the high-temperature region reduce the impact of hydrolysis on the titania phase composition.

The effect of  $\text{H}_2\text{O}/\text{TiCl}_4$  ratio on titania phase composition is illustrated in Figure 8b for powders made by reactant mixing 8 cm from the start of the reactor. As the  $\text{H}_2\text{O}/\text{TiCl}_4$  ratio in the reacting stream was increased, the rutile content decreased. This is clearly observed for powders made at furnace set temperature of 1,673 K. At the higher  $\text{H}_2\text{O}/\text{TiCl}_4$  ratio, more  $\text{TiCl}_4$  is hydrolyzed than oxidized resulting in lower rutile content. This again shows that the hydrolysis product is mostly anatase. These results also are in qualitative agreement with the thermodynamic analysis (Figure 4).

### Aggregate size distributions

Figure 9 shows aggregate particle-size distributions for titania made at 1,473 K furnace set temperature and different  $\text{H}_2\text{O}/\text{TiCl}_4$  ratios. The presence of water vapor leads to a slight

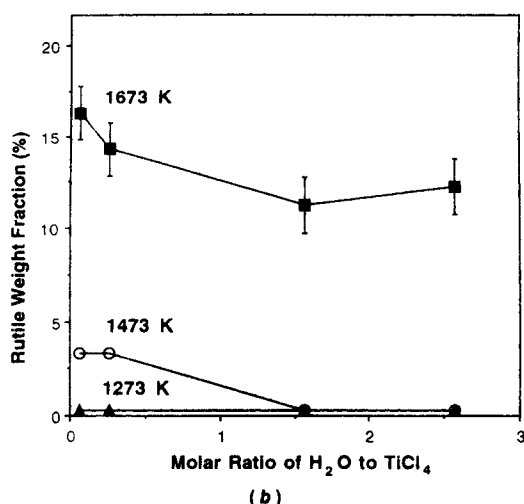
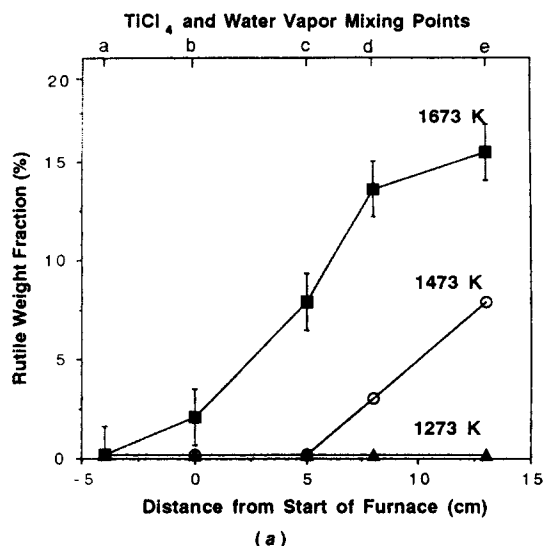


**Figure 8. Rutile content of titania powders made at three furnace set temperatures.**

(a) Different reactant mixing points and a H<sub>2</sub>O/TiCl<sub>4</sub> ratio of 0.26.  
(b) Different H<sub>2</sub>O/TiCl<sub>4</sub> ratios and TiCl<sub>4</sub>-water vapor mixing at 8 cm from the start of the furnace.

increase in aggregate size but varying the H<sub>2</sub>O/TiCl<sub>4</sub> ratio in the process stream has little effect on the aggregate size determined from the DMPS. The same behavior is observed for powders made at 1,273 K, an increase in aggregate size with the introduction of water vapor and no further effect with further increasing H<sub>2</sub>O/TiCl<sub>4</sub> ratios. Changing the mixing point too has little effect on the aggregate size (Table 1). Though

**Table 1. Aggregate Diameter (in  $\mu\text{m}$ ) Measured by the DMPS at Furnace Set Temperature of 1,473 K\***

H <sub>2</sub> O/TiCl <sub>4</sub> Ratio	TiCl <sub>4</sub> and Water Vapor Mixing Points				
	-4 cm	0 cm	5 cm	8 cm	13 cm
0.03	0.21	0.25	0.22	0.25	0.23
0.06	0.21	0.23	0.20	0.23	0.21
0.39	0.20	0.22	0.22	0.24	0.19

\* The mixing points are measured from the start of the furnace and a negative sign indicates mixing of TiCl<sub>4</sub> and water vapor outside the furnace.

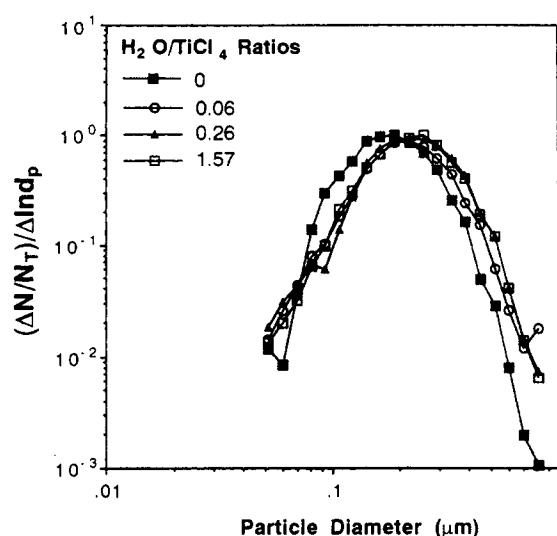


**Figure 9. Aggregate particle-size distributions for titania made at 1,473 K, TiCl<sub>4</sub>-water vapor mixing at the start of the furnace and different H<sub>2</sub>O/TiCl<sub>4</sub> ratios.**

the aggregate size increased with the presence of water, the spread of the distribution remained essentially unchanged between 1.5 and 1.6. Table 1 summarizes the results obtained from the DMPS on aggregate size for powders made at 1,473 K, and at different mixing points and H<sub>2</sub>O/TiCl<sub>4</sub> ratios. The aggregate size for titania made at 1,673 K is quite insensitive to the presence of water and to the temperature at the mixing point.

In all cases, the aggregate size decreased slightly with increasing temperature. The flow rate of the gases was kept constant in all the experiments. With increasing expansion of the gases at higher temperatures, the residence time in the reactor was shorter. Titania particles grow by coagulation. Decreasing residence time leads to a decrease in the time for collision and results in smaller aggregates. For particle growth by coagulation in the free-molecular regime, the diameter of particles increases with residence time as  $t^{1/3}$  while with temperature dependence as  $T^{1/6}$ . This stronger dependence on time leads to slightly smaller aggregates observed on increasing the furnace set temperature which results in shorter reactor residence times. On maintaining constant reactor residence time, Akhtar et al. (1991) found that titania aggregate size increased with temperature due to increased collision frequency among aggregates at higher temperatures.

The average aggregate size obtained from the DMPS was in reasonable agreement with the maximum extent size of the compact aggregates observed under the TEM. For particles made at 1,473 K, mixing TiCl<sub>4</sub> and water vapor 8 cm inside the furnace (at d in Figure 2), and at H<sub>2</sub>O/TiCl<sub>4</sub> ratio of 0.06, the average diameter obtained from the DMPS was 0.23  $\mu\text{m}$  while that measured from TEM micrographs was 0.32  $\mu\text{m}$ . Besides compact aggregates, some long-chainlike aggregates were also observed on the micrographs and the average size of the latter was about 0.6  $\mu\text{m}$ . The DMPS measures an average mobility equivalent diameter which will be closer to the equivalent spherical diameter but smaller than the maximum extent diameter observed on micrographs.

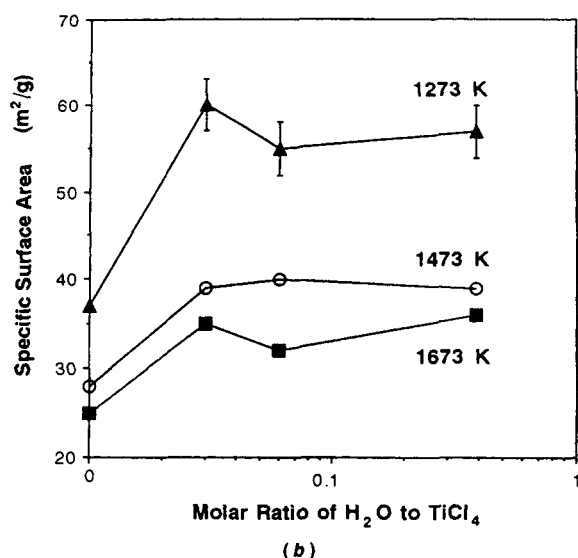
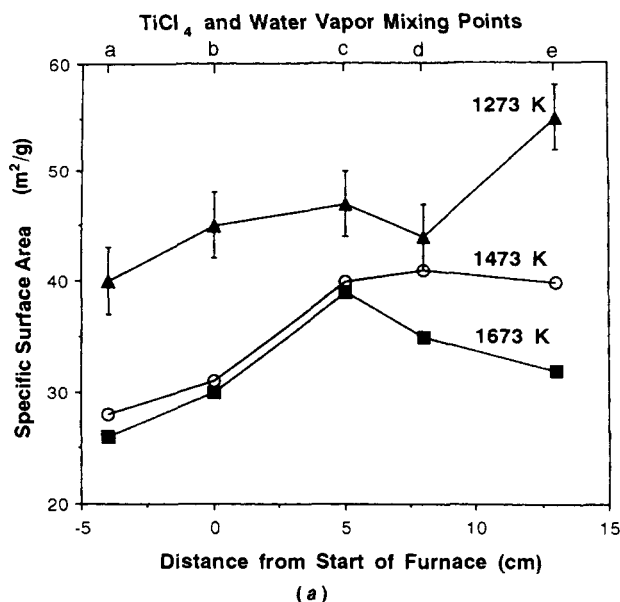


**Figure 10. Specific surface area of titania powders made at different furnace set temperatures.**

(a) Different mixing points of  $\text{TiCl}_4$ -water vapor streams at  $\text{H}_2\text{O}/\text{TiCl}_4$  ratio of 0.06.  
(b) For different  $\text{H}_2\text{O}/\text{TiCl}_4$  ratios and with  $\text{TiCl}_4$ -water vapor mixing 13 cm inside the furnace.

### Specific surface area and aggregate structure analysis

Figure 10a shows the effect of different mixing points on specific surface area of titania particles made at furnace set temperatures of 1,273, 1,473, and 1,673 K and  $\text{H}_2\text{O}/\text{TiCl}_4$  ratio of 0.06. The location of the mixing point of  $\text{TiCl}_4$  and water vapor streams did not significantly affect the specific surface area of the product titania. This was consistent with microscopic observations (Figures 5b and 5c). The average primary particle diameter determined from BET analysis was  $0.05 \mu\text{m}$  for titania made at 1,473 K at a  $\text{H}_2\text{O}/\text{TiCl}_4$  ratio of 0.06 and mixing  $\text{TiCl}_4$  and water vapor at the start of the furnace while the diameter from TEM was  $0.03 \mu\text{m}$ . For powders made at the same conditions but mixing  $\text{TiCl}_4$  and water vapor 8 cm from the start of the furnace (at d in Figure 2) the primary

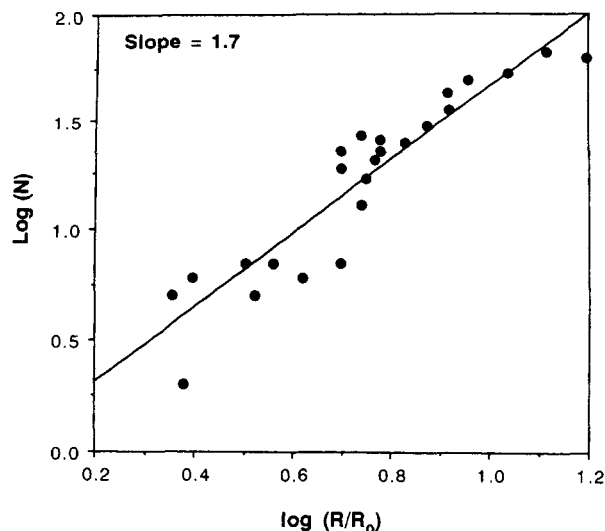


**Figure 11. Logarithmic plot of  $N$  vs.  $(R/R_0)$  for titania made at 1,473 K with  $\text{TiCl}_4$ -water vapor mixing 8 cm from the start of the furnace and  $\text{H}_2\text{O}/\text{TiCl}_4$  ratio of 0.06.**

The slope of this line gives the fractal dimension of the aggregates.

particle diameter from BET surface area measurements was  $0.05 \mu\text{m}$  and that obtained from micrographs was  $0.04 \mu\text{m}$ . In general, the specific surface area of titania decreases with temperature at all mixing points since particles sinter faster at high temperatures.

Figure 10b shows the variation in specific surface area of titania particles (mixing point e, 13 cm inside the furnace) with temperature and  $\text{H}_2\text{O}/\text{TiCl}_4$  ratio. Powders made in the presence of water vapor had a higher specific surface area than those made in the absence of water. The average primary particle diameter (from BET surface area measurements) of titania powders made at 1,473 K was  $0.07 \mu\text{m}$  in the absence of water and  $0.05 \mu\text{m}$  at a  $\text{H}_2\text{O}/\text{TiCl}_4$  ratio of 0.06 and the mixing point at d (8 cm from start of furnace). The corresponding primary particle diameters observed under the TEM were 0.08 and  $0.04 \mu\text{m}$ , respectively. Increasing the  $\text{H}_2\text{O}/\text{TiCl}_4$  ratio in the system had little effect on the specific surface area (Figure 10b). At all temperatures and mixing points, the specific surface area increased with the introduction of water vapor but further increasing the  $\text{H}_2\text{O}/\text{TiCl}_4$  ratio had little effect. Crystallite sizes (obtained from X-ray line broadening) of titania made in the absence of water are larger than those of titania made in the presence of water at constant furnace set temperatures. Changes in  $\text{H}_2\text{O}/\text{TiCl}_4$  ratio have no significant effect on crystallite size. These results agree with specific surface area measurements (Akhtar, 1993).

Readey and Readey (1987) reported significant increase in the grain size of titania sintered in the presence of water vapor though the densification rates were not affected for experiments conducted at 1,573 K for 5 hours. Quantitative modeling shows that the rate-limiting steps that resulted in faster sintering and surface area reduction are the formation of volatile  $\text{Ti}(\text{OH})_2\text{Cl}_2$  and the diffusion of hydroxyl ions (Gruy and Pijolat, 1992). These findings would seem to contradict the present results of high surface area titania being formed on



the introduction of water vapor. However, it should be borne in mind that in the experiments reported here, the presence of water vapor presents an alternative route for  $\text{TiCl}_4$  conversion: hydrolysis. Titania formed by hydrolysis has a higher specific surface area than that formed by oxidation (Clark, 1975). It is the presence of titania made by the hydrolysis route that leads to the increase in specific surface area observed experimentally. If these powders had been further exposed to the 3–5 hours at high temperatures as reported in the literature, then they too would have sintered further and reduced their specific surface area.

Titania made in the presence of water has a larger aggregate size and smaller primary particle size compared to the aggregates made in the absence of water. The relation observed between the aggregate size and primary particle size is consistent with the theoretical predictions of Matsoukas and Friedlander (1991) and their observations on the behavior of zinc oxide and magnesium oxide agglomerates. For large aggregates comprising  $N$  primary particles ( $N \rightarrow \infty$ ), it has been shown by simulations that (Witten and Sander, 1981):

$$N \sim R_g^{D_f} \quad (4)$$

where  $R_g$  is the radius of gyration and  $D_f$  is the mass fractal dimension. Gas-phase synthesized particles are rarely strictly fractal in the strictest sense, but it has been shown that they exhibit a power law behavior (Samson et al., 1987):

$$N \sim (R/R_o)^{D_f} \quad (5)$$

where  $R$  is the collision radius of the aggregate and  $R_o$  is the radius of the primary particle.

The above relation allows determination of the fractal dimension of aggregates from TEM micrographs (Samson et al., 1987). For ease of calculation of a mass fractal dimension, the maximum extent of the TEM image of the aggregate particle was used for  $R$ . Details of the image and data analysis can be found in Akhtar (1993). Slopes of logarithmic plots of  $N$  vs.  $R$  give the fractal dimension (Figure 11). For particles made at 1,273 K, the fractal dimension was 1.5, increased to 1.7 for particles made at 1,473 K and to 1.9 for particles made at 1,673 K. The differences in fractal dimension is an indication of faster primary particle growth at higher temperatures due to higher rates of sintering.

## Conclusions

The effect of water vapor on titania particle characteristics and the competition between  $\text{TiCl}_4$  oxidation and hydrolysis was experimentally investigated. Low-temperature mixing of the  $\text{TiCl}_4$  and water vapors makes hydrolysis dominant resulting in the formation of round anatase particles. As the temperature of mixing of the two streams is increased, the particles become polyhedral with well defined edges and their rutile content increases while the specific surface area and crystallite size remain virtually unchanged. The presence of water vapor reduces the rutile content. Structural analysis of aggregates observed on TEM showed an evolution of the fractal dimension from 1.5 for particles made at 1,273 K to 1.9 for particles made at 1,673 K.

## Acknowledgment

This research was supported by the National Science Foundation, Grant CTS-8908197 and E. I. DuPont de Nemours and Co. Inc. The authors wish to thank the Department of Geology and the Department of Materials Science and Engineering at the University of Cincinnati for use of their X-ray diffractometer.

## Literature Cited

- Akhtar, M. K., Y. Xiong, and S. E. Pratsinis, "Vapor Synthesis of Titania Powder by Titanium Tetrachloride Oxidation," *AIChE J.*, **37**, 1561 (1991).
- Akhtar, M. K., S. E. Pratsinis, and S. V. R. Mastrangelo, "Effect of Dopants in Vapor Synthesis of Titania Powders," *J. Amer. Ceram. Soc.*, **75**, 3408 (1992).
- Akhtar, M. K., "Role of Additives in Vapor Phase Synthesis of Titania," PhD Thesis, Univ. of Cincinnati (1993).
- Bankmann, M., R. Brand, B. H. Engler, and J. Ohmer, "Forming of High Surface Area  $\text{TiO}_2$  to Catalyst Supports," *Catal. Today*, **14**, 225 (1992).
- Bautista, J. R., and R. M. Atkins, "The Formation and Deposition of  $\text{SiO}_2$  Aerosols in Optical Fiber Manufacturing Torches," *J. Aerosol Sci.*, **22**, 667 (1991).
- Chen, C.-J., and J.-M. Wu, "The Effect of Niobium, Calcium and Lanthanum Dopants on the Crystallite Growth of  $\text{TiO}_2$  Powders," *Mat. Sci. Eng.*, **B5**, 377 (1990).
- Clark, H. B., "Titanium Dioxide Pigments," *Pigments*, Part 1, R. R. Myers and J. S. Long, eds., Marcel Dekker, New York (1975).
- Gruy, F., and M. Pijolat, "Kinetics of Anatase  $\text{TiO}_2$  Surface Area Reduction in a Mixture of  $\text{HCl}$ ,  $\text{H}_2\text{O}$ , and  $\text{O}_2$ : II. Quantitative Modeling," *J. Amer. Ceram. Soc.*, **75**, 663 (1992).
- Hebrard, J., P. Nortier, M. Pijolat, and M. Soustelle, "Initial Sintering of Submicrometer Titania Anatase Powder," *J. Amer. Ceram. Soc.*, **73**, 79 (1990).
- Klug, H. P., and L. E. Alexander, *X-Ray Diffraction Procedures*, Wiley, New York, Chap. 9 (1954).
- Kumar, K. P., V. T. Zaspalis, F. F. M. De Mul, K. Keizer, and A. J. Burggraaf, "Thermal Stability of Supported Titania Membranes," *Better Ceramics Through Chemistry: V. Mat. Res. Soc. Symp. Proc.*, Vol. 271, M. J. Hampden-Smith, W. G. Klemperer, and C. J. Brinker, eds., 499 (1992).
- Lide, D. R., ed., *CRC Handbook of Chemistry and Physics*, CRC Press, Boca Raton, FL, p. 4 (1990).
- Lyons, S. W., Y. Xiong, T. L. Ward, T. T. Kodas, and S. E. Pratsinis, "Role of Particle Evaporation during Synthesis of Lead Oxide by Aerosol Decomposition," *J. Mat. Res.*, **7**, 3333 (1992).
- Matsoukas, T., and S. K. Friedlander, "Dynamics of Aerosol Agglomerate Formation," *J. Coll. Interf. Sci.*, **146**, 495 (1991).
- Mezey, E. J., "Pigments and Reinforcing Agents," *Vapor Deposition*, C. F. Powell, J. H. Oxley, and J. M. Blocher, Jr., eds., Wiley, New York, p. 423 (1966).
- Ollis, D. F., E. Pelizzetti, and N. Serpone, "Photocatalytic Destruction of Water Contaminants," *Environ. Sci. Tech.*, **25**, 1523 (1991).
- Oguri, Y., R. E. Riman, and H. K. Bowen, "Processing of Anatase Prepared from Hydrothermally Treated Alkoxy-derived Hydrous Titania," *J. Mat. Sci.*, **23**, 2897 (1988).
- Perkin Elmer Handbook of X-ray Photoelectron Spectroscopy*, Perkin Elmer (1978).
- Pratsinis, S. E., H. Bai, P. Biswas, M. Frenklach and S. V. R. Mastrangelo, "Kinetics of  $\text{TiCl}_4$  Oxidation," *J. Amer. Ceram. Soc.*, **73**, 2158 (1990).
- Rao, C. N. R., S. R. Yoganarashimhan, and P. A. Faeth, "Studies on the Brookite-Rutile Transformation," *Trans. Farad. Soc.*, **57**, 504 (1961).
- Readey, M. J., and D. W. Readey, "Sintering  $\text{TiO}_2$  in  $\text{HCl}$  Atmospheres," *J. Amer. Ceram. Soc.*, **70**, C358 (1987).
- Reynolds, W. C., "STANJAN—Interactive Computer Programs for Chemical Equilibrium Analysis," Dept. Mech. Eng., Stanford Univ. (1987).
- Samson, R. J., G. W. Mulholland, and J. W. Gentry, "Structural Analysis of Soot Agglomerates," *Langmuir*, **3**, 272 (1987).

Shannon, R. D., and J. A. Pask, "Topotaxy in the Anatase-Rutile Transformation," *Amer. Mineralogist*, **49**, 1707 (1964).  
Spurr, R. A., and H. Myers, "Quantitative Analysis of Anatase-Rutile Mixtures with an X-Ray Diffractometer," *Analy. Chem.*, **29**, 760 (1957).  
Suyama, Y., and A. Kato, "Effect of Additives on the Formation of

TiO<sub>2</sub> Particles by Vapor Phase Reaction," *J. Amer. Ceram. Soc.*, **68**, C154 (1985).  
Witten, T. A., and L. M. Sander, "Diffusion-Limited Aggregation, a Kinetic Critical Phenomenon," *Phys. Rev. Lett.*, **47**, 1400 (1981).

*Manuscript received Sept. 2, 1993.*

---